NOTES AND CORRESPONDENCE

A Comparison of Vertical Eddy Mixing Parameterizations for Equatorial Ocean Models

NEVILLE R. SMITH AND G. DALE HESS

Bureau of Meteorology Research Centre, Melbourne, Victoria, Australia

30 August 1991 and 17 March 1992

ABSTRACT

The vertical eddy mixing formulations employed in the K-theory model of Pacanowski and Philander and in second-moment closure models are compared for an equatorial Pacific Ocean simulation. The Pacanowski and Philander model is found to be mainly driven by changes in the stratification rather than shear-generated instabilities, and the position and width of the mixing transition zone between high and low mixing values is found to be sensitive to the parameters of the model. In the second-moment closure models the master length scale limit effectively determines the threshold of the mixing zone, while the inclusion of storage, advection, and diffusion terms in the turbulent kinetic energy equation affects both the position and extent of the transition zone. Viscous mixing is more intense than diffusive mixing in the Pacanowski and Philander scheme, but in the second-moment closure models the reverse tends to be true. As expected, there is no simple functional relationship between the gradient Richardson number and the intensity of mixing in the second-moment closure schemes.

1. Introduction

The aim of the present study is to compare the commonly used K-theory vertical mixing model of Pacanowski and Philander (1981, hereafter PP) with a turbulent closure model. The former model has been widely adopted in the oceanographic community as a simple, but effective, parameterization of vertical mixing in the tropical regions (Philander and Seigel 1985; Latif et al. 1988; Giese and Harrison 1990). Its important virtues are that it may be tuned to give reasonably realistic equatorial flow and temperature regimes and it offers manageable parameter freedom. The latter approach is here represented by the Mellor and Durbin (1975) and Mellor and Yamada (1982) higher-order turbulent closure model, hereafter referred to as second-moment closure (SMC; Mellor 1989). SMC models have strong theoretical and empirical foundations and are sufficiently general not to require special tuning for different situations. Such models have been applied in a wide variety of oceanic situations (Mellor and Yamada 1982; Martin 1985; Mellor 1989). The turbulence balance is local in nature but can include three-dimensional advection and diffusion of turbulent kinetic energy. The appeal of the SMC models lies in their generality but at a cost of increased complexity, and this needs to be balanced against the simplicity and effectiveness of the empirical approach. This study concentrates on building an understanding of the relationship between these two approaches and on understanding some of the sensitivities of the parameterizations.

The PP model and the SMC models have been adopted in several tropical oceanic circulation studies, but an extensive three-dimensional intercomparison has yet to be done, and there has not been any systematic attempt to understand the ramifications of various assumptions implicit in the models in the context of large-scale tropical ocean circulation. Pacanowski and Philander discussed some of the implications of the adjustable parameters in their formulation. For the SMC schemes we will examine the implications of the level of closure and other aspects of the implementation within the context of equatorial ocean modeling. We will then attempt to define the relationship between the two approaches and, in particular, to place the PP approach in the context of the more general SMC schemes.

2. Vertical mixing in a Pacific Ocean model

The test bed here is a Pacific Ocean model similar to Philander and Seigel (1985). The domain extends from 130°E to 72°W zonally and from 30°S to 38°N in latitude. The resolution is fixed at 2° zonally but varies in the meridional direction (symmetrically about the equator) from 0.5° in the equatorial region to 3° at high latitudes. There are ten approximately equally spaced levels down to 150 m and a further ten levels of increasing thickness to the bottom at 3000 m. This resolution is the best compromise that we could make given the limited resources at our disposal. The code

Corresponding author address: Dr. Neville R. Smith, Bureau of Meteorology Research Centre, GPO Box 1289K, Melbourne, Victoria, 3001, Australia.

has been adapted from the GFDL Modular Ocean Model Version 1.0 (MOM 1.0; Pacanowski et al. 1991). (The actual code used for these experiments is based on a preliminary release of MOM 1.0 but can be considered as equivalent for the present purposes.)

Many of the earlier numerical models for the tropical ocean circulation assumed the vertical eddy mixing coefficients were constant (Philander and Pacanowski 1980; Latif 1987), but the simulations usually suffered from poor equatorial undercurrent (EUC) and thermocline representations. Pacanowski and Philander (1981) proposed an alternative representation specifically tuned for numerical models of the tropical circulation in which the vertical mixing could be parameterized in terms of the shear and buoyancy of the large-scale flow,

$$\nu = \frac{\nu_N}{(1 + \alpha \mathrm{Ri})^n} + \nu_b, \quad \kappa = \frac{\nu}{(1 + \alpha \mathrm{Ri})} + \kappa_b, \quad (1)$$

where ν_b and κ_b are background dissipation parameters, ν_N, α, and n are adjustable parameters (ν_N is, in effect, the mixing coefficient under neutral conditions), $\mathrm{Ri} = N^2/[(\partial u/\partial z)^2 + (\partial v/\partial z)^2]$ is the gradient Richardson number, $N^2 = -g/\rho_0 \times \partial\rho/\partial z$ is the square of the Brunt–Väisällä frequency, and g is the gravitational acceleration. Pacanowski and Philander found that the equatorial thermocline and EUC were best simulated using $\nu_b = 1 \times 10^{-4}$ m^2 s^{-1}, $\kappa_b = 1 \times 10^{-5}$ m^2 s^{-1}, $n = 2$, $\alpha = 5$, and $\nu_N = \mathrm{O}(50 \times 10^{-4}$ m^2 s$^{-1})$. This parameterization has been widely adopted in studies of the equatorial ocean circulation (Philander and Seigel 1985; Latif et al. 1988; Giese and Harrison 1990) but often with slight variations on the suggested parameter values. For example, Latif et al. (1988) use values of 2×10^{-3} m^2 s^{-1}, 1×10^{-5} m^2 s^{-1}, and 1×10^{-6} m^2 s^{-1} for the neutral viscosity ν_N and the background viscosity and diffusion ν_b and κ_b, respectively. Peters et al. (1988) obtained profiles of velocity, density, and microstructure near the equator at 140°W in the Pacific Ocean in order to estimate Richardson numbers, turbulent dissipation rates, and vertical eddy coefficients. They fit the model described by (1) to their mean Richardson number and vertical eddy mixing coefficients, and obtained estimates of 1.5, 5×10^{-4} m^2 s^{-1}, 2×10^{-5} m^2 s^{-1}, and 1×10^{-6} m^2 s^{-1} for n, ν_N, ν_b, and κ_b, respectively, as long as Ri > 0.25. For Ri near 1/4 the eddy coefficients rose far more sharply as the Richardson number decreased. For the present study we use the values suggested by PP.

The theory and observational verification for various SMC models are described in a number of papers (for example, Mellor and Yamada 1974; Mellor and Durbin 1975; Mellor and Yamada, 1982; Mellor 1985, 1989). Here, we shall examine two versions of SMC models, namely, the so-called level 2 and level 2½ models (Mellor and Yamada 1982). The implementation of the level 2½ model follows the derivation discussed in Rosati and Miyakoda (1988) (as formulated in MOM 1.0), while the level 2 model is derived from Mellor and Yamada (1982). The vertical mixing coefficients are written as

$$\nu = lqs_M + \nu_b, \quad \kappa = lqs_H + \kappa_b, \quad (2)$$

where $\frac{1}{2}q^2$ is the turbulent kinetic energy (TKE), l is the master turbulence length scale, s_M and s_H are stability functions, and ν_b and κ_b are again background mixing rates (Mellor and Yamada 1982). The solution for q proceeds in different ways depending upon the level of closure. For level 2 the local time change, advection, and diffusion of TKE are ignored, and shear and buoyant production are balanced against the dissipation of TKE; q is then obtained algebraically as a function of the Richardson number. At level 2½ the full TKE equation is stepped forward in time in a manner analogous to the tracer equations. The solution for l may be obtained algebraically (Blackadar 1962; Mellor and Yamada 1974) or by time stepping a differential equation (Mellor and Yamada 1982; Rosati and Miyakoda 1988). While the latter form is somewhat empirical, it does appear to give better results (Mellor 1989) and would seem better suited to the presumably significant variation in l across the EUC. We test both implementations here.

Our consideration of the SMC implementation is restricted to variations that appear to produce effects analogous to those produced by variations in the parameters of the PP scheme. One such variation arises through the need to restrict the vertical size of eddies in a stably stratified fluid so that the local dissipation length is determined locally by the TKE level and the Brunt–Väisällä frequency N (Deardorff 1976):

$$l_{\max} = \alpha_l^* \frac{q}{N}. \quad (3)$$

While (3) is physically reasonable, there is considerable uncertainty in choosing the value of α_l^*. Rosati and Miyakoda (1988), following Galperin et al. (1988), suggest a value of 0.53. Sykes et al. (1988) used a value of 1.0, while the default value in MOM 1.0 is 0.1.

3. Mixing regimes and model results

The principal aim of this study is to provide a suitable context for the meaningful comparison and evaluation of vertical mixing parameterizations in three-dimensional tropical ocean climate simulations. The effect of vertical mixing parameterizations is not confined locally, but through the various feedbacks on the oceanic circulation as a whole, can influence the mixing regimes at remote sites. It is difficult then to delineate cause and effect since the cause of changed mixing at a site may be due to changes in the strength or structure of the large-scale circulation pattern. One-dimensional local mixing theory arguments are no longer satisfac-

tory. For the mixing states, a myriad of cross sections and maps of mixing rates, kinetic energy, shear and buoyancy production rates, and Richardson number are available, all with complex spatial and temporal structure. We learned very quickly, however, that such data could not tell us *how* the various schemes worked, nor could they yield insight into the relationships between the various formulations for vertical mixing. Instead, several alternative ways to visualize the mixing processes are presented.

A useful view of the mixing regime is provided by mapping the Richardson number and vertical eddy mixing coefficients in the shear-buoyancy plane (Fig. 1). For PP and the level 2 closure models, at least, this is relatively straightforward. For much of the PP regime (Fig. 1b) the eddy viscosity is close to the background values (the diffusion maps are similar and are not shown). As the shear increases and/or the buoyancy decreases, the (parameterized) vertical mixing increases, changing most rapidly near Ri = 0.1. Thereafter, the rate of change with increasing shear and/or decreasing buoyancy tapers off, approaching the so-called neutral condition limit. For the corresponding maps at level 2 closure we assume a single level of 50 m, with TKE fixed by the surface boundary condition, and then calculate l, eddy viscosity, and eddy diffusivity as functions of shear and buoyancy at 25 m. Figure 1c shows the case where $\alpha_l^* = 1$. Again note that the plane is divided into background and active mixing zones for both eddy viscosity and diffusivity, but now the intermediate region is more compact. The change from background to active mixing is relatively rapid, tending to, but not exactly, follow decreasing Richardson number.

If α of the PP scheme (Fig. 1d) is varied, we find that the entire pattern is shifted toward low (high) gradient Richardson numbers as α is increased (decreased), with no change in the pattern itself. If n is varied, the pattern remains in about the same place (Fig. 1e), but the pattern is expanded (contracted) as n is decreased (increased). While the neutral and background mixing rates are important for the ocean circulation simulation, as shown by PP, both α and n are important in determining the structure and sensitivity of mixing to the mean state. If the level 2 master length limit as defined by (3) is varied ($\alpha_l^* = 0.1$; Fig. 1f), we find a significant shift in the location of the transition zone between the background and active mixing parts of shear-buoyancy plane. Note that the intermediate zone of the PP scheme is everywhere within the background zone of this parameterization. So, lowering the value of α_l^* in SMC tends to have a similar effect to increasing values of α in the PP scheme.

While the above technique is useful for relating the simpler parameterizations, it is of limited value when the TKE equation is no longer algebraic as, for example, in the level 2½ closure models. To continue the comparison we use data sampled from four different runs of the Pacific Ocean model, each integrated to a seasonal equilibrium:

(*i*) a model using PP with parameters as described in section 2
(*ii*) a level 2 SMC model with $\alpha_l^* = 0.1$
(*iii*) a level 2½ SMC model with $\alpha_l^* = 0.1$ and l determined algebraically
(*iv*) a level 2½ SMC model with $\alpha_l^* = 0.1$ and the l equation.

This choice for α_l^* effectively reduces the critical Richardson number at which mixing emerges, perhaps overly so, but is adopted because it is the default value in MOM 1.0. For each of these cases the shear, buoyancy, and vertical eddy coefficients were extracted along representative vertical sections for December of the final year of the seasonal integration and then plotted as points in a shear-buoyancy plane, with the size of the dot linearly related to the magnitude of the eddy mixing coefficient.

The results for the PP model (Fig. 2a) correspond well with the parameter dependence forecast by Fig. 1. The majority of values are in the background zone, with a smaller number occupying the transition zone and almost none in the active mixing zone. The higher values tend to be in the low buoyancy–moderate shear portion of the plane rather than in the high-shear zone, suggesting that stratification, and not shear instability, is the dominating factor. The relationship with Richardson number is monotonic as required by (1). Figure 2b shows a similar scatterplot for the level 2 experiment. The number of active mixing points is lower than in the PP model. There are now background mixing points interspersed with the active mixing points, and the mixing points are now scattered into the high-shear portion of the plane. There appear to be fewer intermediate values in comparison with the PP run.

In the level 2½ SMC experiments (Figs. 2c and 2d) by far the majority of points belong to the background mixing group, but there are now many active points with widely varying mixing rates, particularly when compared with the level 2 scheme. There is no tendency toward an on–off mixing dependency and the distribution of mixing is somewhat more closely aligned with Richardson number. There is no direct relationship between the level of mixing and Ri. As α_{l^*} is increased, the threshold of mixing moves to higher Richardson numbers (not shown). Note that the "fanning out" of the mixing isolines at low buoyancy and low shear as shown in Fig. 1b is also apparent in the higher-level models. The precise role played by the differential equation for l is not at all clear from these diagrams. Figure 2d shows that the mixing tends to be shifted slightly toward higher Richardson numbers and to be marginally more constrained (compared to Fig. 2c). Perhaps the most noteworthy characteristic of Fig. 2d is its similarity to the PP scheme (Fig. 2a).

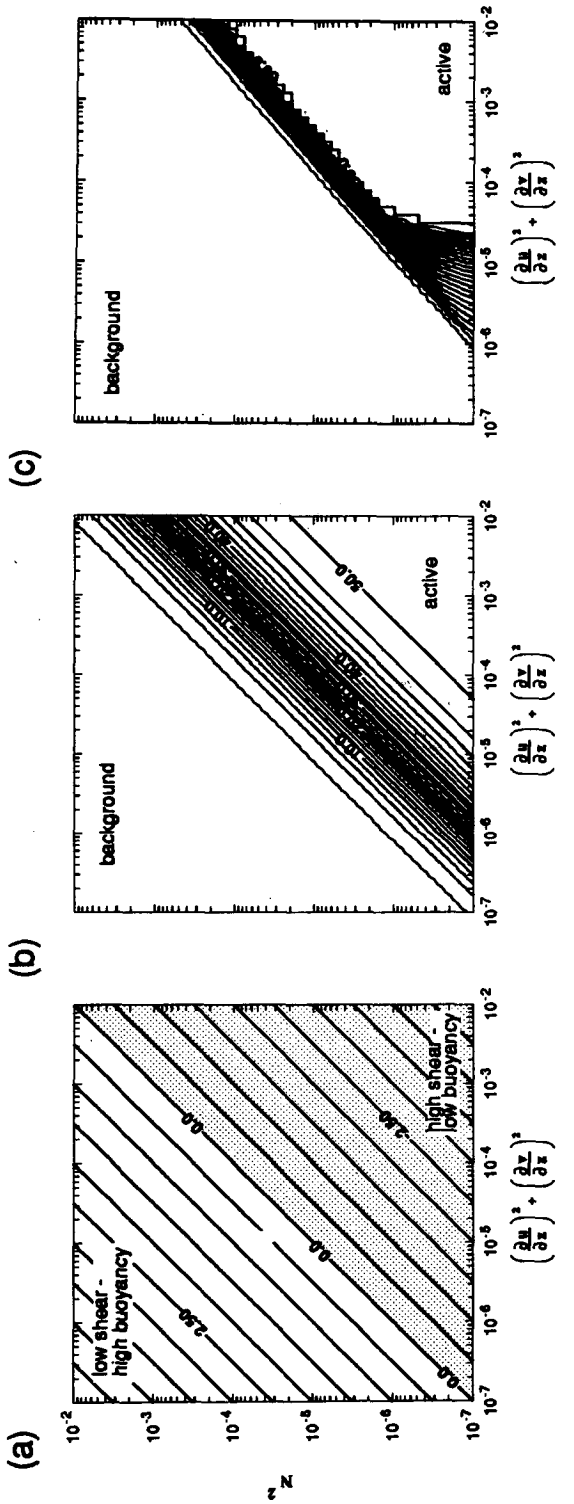

FIG. 1. (a) Plot of the variation of $\log_{10}$Ri as a function of the mean-flow shear and buoyancy. Both axes are transformed into $\log_{10}$ dependencies. In this frame of reference, lines of constant $\log_{10}$Ri are straight lines, and the variation from high buoyancy–low shear (top left) to low buoyancy–high shear (bottom right) is constant. Values of Ri less than unity are shaded. (b) Vertical eddy viscosity in the PP scheme (units: $\text{cm}^2\,\text{s}^{-1}$). (c) As in (b) but for level 2 SMC and $\alpha_1^* = 1.0$. (d) As in (b) but with $\alpha = 0.5$. (e) As in (b) but with $n = 1$. (f) As for (c) but with α_1^* reduced to 0.1.

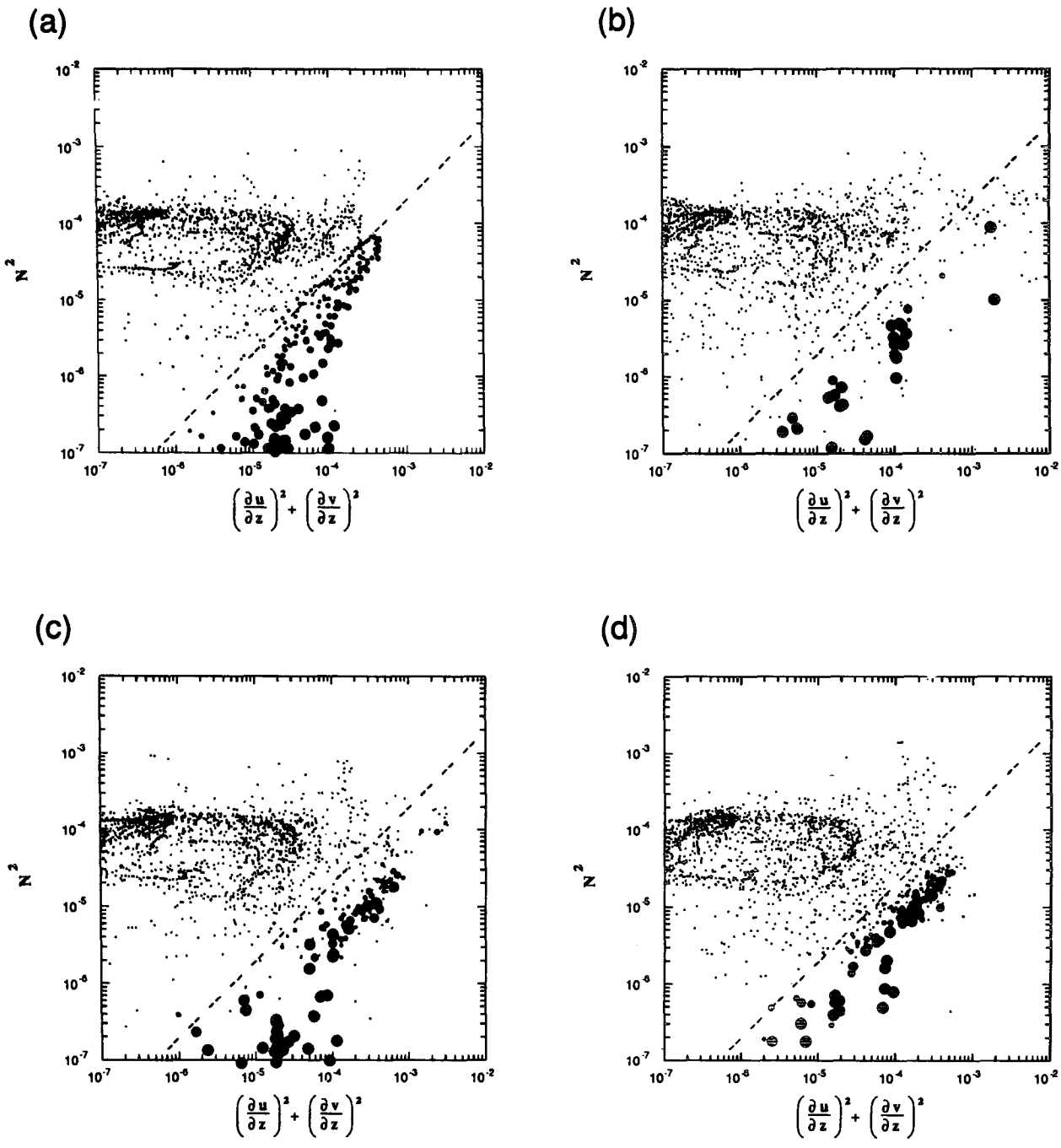

FIG. 2. Scatterplot of shear-buoyancy realizations from (a) the Pacanowski and Philander model, (b) the level 2 closure model with $\alpha_l^* = 0.1$, (c) the level 2½ closure model with $\alpha_l^* = 0.1$ and the algebraic l equation, and (d) the level 2½ closure model with $\alpha_l^* = 0.1$ and the differential l equation. The scatter samples are taken from a "snapshot" of three top-to-bottom sections, along the equator, 12°N, and 150°W, for the final month of a seasonally forced integration. The smallest dots correspond to the background mixing rate ν_b. The largest dots correspond to the (neutral) limit of the mixing, ν_N. The dashed line marks Ri = 0.195, the threshold of mixing in the level 2 second-moment closure scheme. The axes are as in Fig. 1.

Pacanowski and Philander concluded that the EUC strength is sensitive to the eddy viscosity assigned under neutral conditions. In Fig. 1, any change in the magnitude of the neutral condition eddy mixing coefficient would result in a rescaling of the contours but would not entail any changes in the location or structure of the pattern. For a given vertical profile, a smaller α would in effect introduce mixing at higher values of

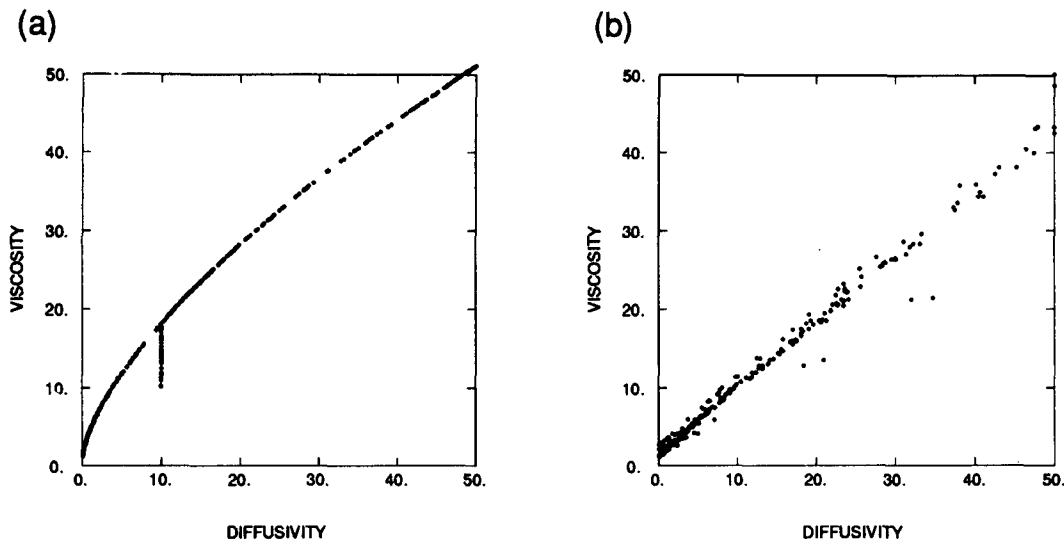

FIG. 3. A scatterplot of the eddy viscosity against the eddy diffusivity for (a) experiment (i) and (b) experiment (iv) (see text and Fig. 2). The units are centimeters squared per second. The majority of points are coincident at (1.0, 0.1) in the ν–κ plane. Note that the PP scheme is implemented with a minimum mixing in the surface level of 10 cm^2 s^{-1} to take account of the direct contribution by wind mixing.

Ri and, in view of the usual increase in Ri with depth, would cause active mixing to penetrate deeper on average. An increase in n, for the same profile, would shrink the transition zone from low to high mixing. If we adopt the terminology of the bulk mixed layer approach, then α affects the depth of the mixed layer, while n affects the sharpness of the change between the mixed layer and the quiescent waters beneath.

These inferences do seem, at first glance, to be at odds with the results of PP. It should be borne in mind, however, that the circumstances of their evaluation (the response to impulsive zonal winds) is rather different from the present case (the equilibrium response under seasonal forcing). They found that variations in α and n alter the speed but not the shear (of an eastward jet) and that the sensitivity to changes in ν_N was greatly reduced once surface heating was applied. Our experience is consistent with the latter finding but suggests the α and n can be important.

In the SMC models we do not have a similar direct control on the relationship between the mixing rates and the mean-flow shear and buoyancy. We do, however, have some flexibility in parameterizations that control the penetration of TKE vertically and the determination of the master length scale. The SMC models are more tightly constrained in respect to the Ri threshold for active mixing, unlike the PP scheme where this threshold is simply a function of adjustable parameters. For the level 2 models an equivalent "tuning" comes in the form of a constraint (3) on the (algebraically determined) master length scale under stable conditions. Developing the mixed layer analogy above, a smaller value of α_l^* leads to an effective shift of the Ri threshold to lower values of Ri, thus reducing the depth of the mixed layer. There is no obvious counterpart to n in the SMC schemes. In the level 2½ SMC model vertical advection and diffusion of TKE tend to smooth the transition from low to high mixing. The addition of an l equation appears to resharpen the transition zone. It is not clear whether this is due to local effects, such as vertical advection, or through horizontal transport of information.

In the PP scheme the viscosity ν is always greater than the diffusion κ for stable or neutral conditions, as required by (1) (Fig. 3a). For the SMC models this relationship is less straightforward because of the complicated dependence of the stability functions on the shear, buoyancy, and l. Figure 3b shows the relationship in the level 2½ model. The data are exactly the same as those used to construct the scatterplots of Fig. 2.[1] The diffusion mixing rates are nearly equal to, or possibly greater than, the viscous mixing rates, which is the reverse of the dependence found for the PP scheme. The extrapolation of Fig. 3b to neutral stability suggests a Prandtl number of around 0.8 consistent with Mellor and Yamada (1982). The neutral limit of PP is approximately 1.

[1] In the present implementation of PP, ν and κ are estimated from Ri calculated at velocity and temperature points, respectively, so the relationship implied by (1) may be contaminated by grid-scale noise. SMC is implemented in a way that uses a single estimation of the shear and buoyancy (at temperature points), but the production terms and final estimation of the mixing coefficients involve several interpolations, which again serve to introduce noise into the ν–κ relationship. We overcome this in Fig. 3 by extending the integrations over several time steps with a self-consistent arrangement. These problems may need to be addressed in future implementations of the model.

The relationship between the mixing rates and Ri is one-to-one in the PP scheme as required by the formulation (1) (Fig. 4a). The level 2 and level 2½ cases are less straightforward (Figs. 4b and 4c). In the level 2 example the threshold of mixing is shifted, and the transition from low to high mixing is much sharper, as noted previously. The relationship between viscosity and Richardson number is not one-to-one, and there is considerable scatter, the points tending to lie at one mixing extreme or the other. There is more consistency in the level 2½ distribution. Once more, the relationship is not one-to-one, with a broad scatter of points, perhaps favoring the low-mixing part of the range. The transition is still relatively rapid, although for the most sophisticated case (Fig. 4c) there is more of a tendency for the active mixing to ramp in gradually. In this latter case there is a greater profusion of points at the low end of the active mixing range.

Archer (1990) commented that the SMC models essentially operated as Richardson number–driven schemes, based principally on intercomparisons with the level 2 model in one-dimensional simulations. The present experimental results suggest a more complex relationship. The reason for this disparity may be due in part to the different context of the evaluation. Mixing schemes are often evaluated at sites where abundant data are available over a long period in time, with the implicit assumption being that horizontal advection/diffusion of information is not important. In the present case these effects cannot be ignored. Of the models considered here the level 2 SMC approach is the least suited since it has neither the parameter flexibility of the PP approach nor the sophistication of higher-level SMC. In the latter models there are feedbacks between l and the intensity of mixing, three-dimensional diffusion, and advection of both TKE and l, all of which tend to overwhelm any simple functional dependence of the mixing rates on Ri.

4. Conclusions

From the results and discussion presented here, we are led to the following conclusions.

- The Pacanowski and Philander (1981) scheme provides a capability for tuning the strength and vertical structure of the equatorial current system. The parameter α sets the position of the transition region in the shear-buoyancy plane (increased α shifts the mixing toward lower Richardson numbers) and thus determines the effective depth of the surface high-mixing zone. The parameter n determines the width of the transition zone, so that smaller values of n will lead to a more gradual change between the high-mixing and background-mixing regimes.
- The methodology of the level 2 and 2½ SMC schemes is not commensurate with direct tuning of the response but does permit indirect adjustment through various lower-level constraints. The factor α_l^* in the stratified limit to the master length scale determination plays a similar role to α in the Pacanowski and Philander (1981) scheme but with the reverse sense; that

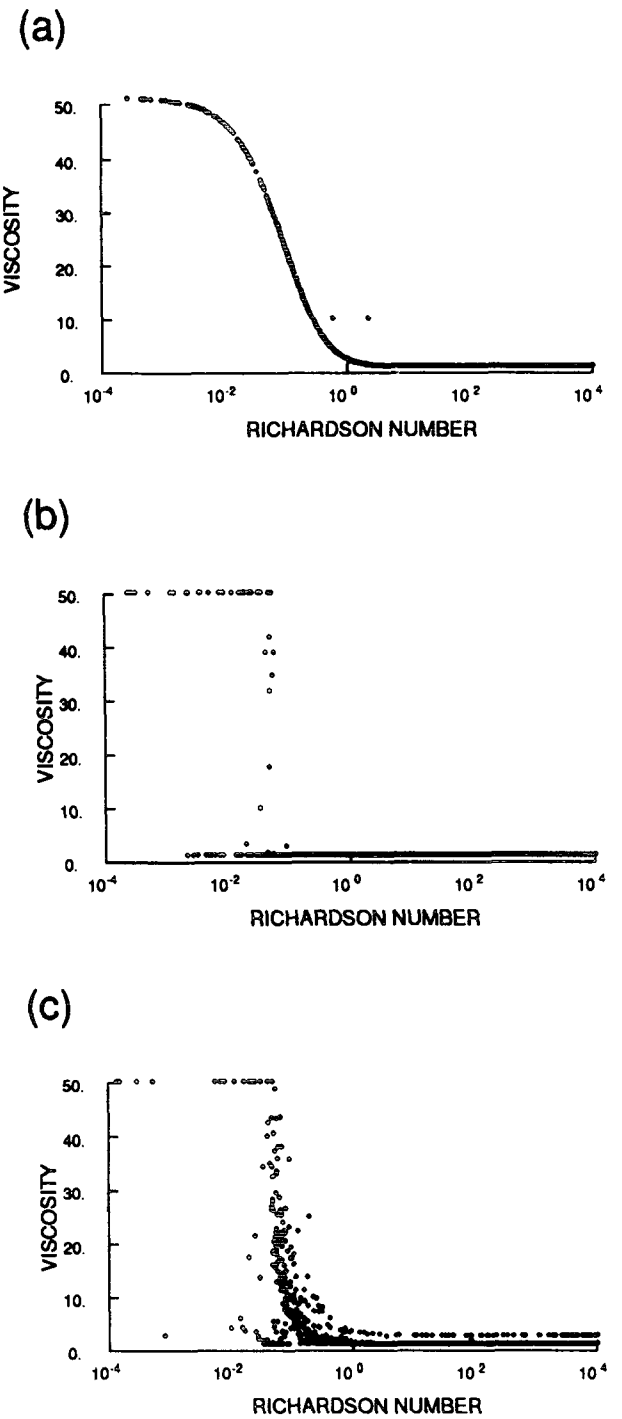

FIG. 4. A scatterplot of the eddy viscosity against the gradient Richardson number for (a) experiment (i), (b) experiment (ii), and (c) experiment (iv) (see text and Fig. 2). The abscissa is transformed using $\log_{10}$.

is, a reduction in α_l^* shifts the transition region in the shear-buoyancy plane to smaller Richardson numbers.

- The addition of the differential equation for TKE (that is, the change from level 2 to 2½ closure) and the inclusion of a differential equation for l significantly alters the mixing regime. The mixing regime in the case with both the TKE and l differential equations is, somewhat surprisingly, quite similar to that of the PP scheme.
- The Pacanowski and Philander scheme ensures that viscosity is greater than diffusion, but the SMC schemes results in near equality, with a tendency toward greater diffusive rates.
- There is no simple functional relationship between the gradient Richardson number and the level of mixing in either the level 2 or level 2½ models.

Acknowledgments. This work would not have been possible without the generosity of the GFDL ocean modeling group who supplied the basic model, first through the efforts of Mike Cox, and lately through Keith Dixon, Ron Pacanowski, and Tony Rosati. We are grateful for this contribution. This paper benefited from the helpful comments of Andrew Moore and Chris Reason.

REFERENCES

Archer, D., 1990: Modelling pCO_2 in the upper ocean: A review of relevant physical, chemical, and biological processes. U.S. Department of Commerce, 65 pp. [NTIS TR050.]

Blackadar, A. K., 1962: The vertical distribution of wind and turbulent exchange in a neutral atmosphere. *J. Geophys. Res.*, **67,** 3095–3102.

Deardorff, J. W., 1976: Clear and cloud-capped mixed layers. Their numerical simulation, structure and growth and parameterization. *Seminars on "The Treatment of the Boundary layer in Numerical Weather Prediction,"* European Centre for Medium-Range Weather Forecasts, Reading, United Kingdom, 234–284.

Galperin, B., L. H. Kantha, S. Hassid, and A. Rosati, 1988: A quasi-equilibrium turbulent energy model for geophysical flows. *J. Atmos. Sci.*, **45,** 55–62.

Giese, B. S., and D. E. Harrison, 1990: Aspects of the Kelvin wave response to episodic forcing. *J. Geophys. Res.*, **95,** 7289–7312.

Latif, M., 1987: Tropical ocean circulation experiments. *J. Phys. Oceanogr.*, **17,** 246–263.

——, J. Biercamp, and H. von Storch, 1988: The response of a coupled ocean–atmosphere general circulation model to wind bursts. *J. Atmos. Sci.*, **45,** 964–979.

Martin, P. J., 1985: Simulation of the mixed layer at OWS November and Papa with several models. *J. Geophys. Res.*, **90,** 903–916.

Mellor, G., 1985: Ensemble average, turbulence closure. *Advances in Geophysics,* Vol. 28, Part B, B. Saltsman and S. Manabe, Eds., Academic Press, 432 pp.

——, 1989: Retrospective on oceanic boundary layer modeling and second moment closure. *Proc. of the 'Aha Huliko'a Hawaiian Winter Workshop on Parameterization of Small-Scale Processes,* Honolulu, Hawaii Institute of Geophysics, 251–272.

——, and T. Yamada, 1974: A hierarchy of turbulence closure models for planetary boundary layers. *J. Atmos. Sci.*, **31,** 1791–1806. (Corrigenda, 1977, *J. Atmos. Sci.*, **34,** 1482.)

——, and P. A. Durbin, 1975: The structure and dynamics of the ocean surface mixed layer. *J. Phys. Oceanogr.*, **5,** 718–728.

——, and T. Yamada, 1982: Development of a turbulence closure model for geophysical fluid problems. *Rev. Geophys. Space Phys.*, **20,** 851–875.

Pacanowski, R. C., and S. G. H. Philander, 1981: Parameterization of vertical mixing in numerical models of tropical oceans. *J. Phys. Oceanogr.*, **11,** 1443–1451.

——, K. Dixon, and A. Rosati, 1991: The GFDL Modular Ocean Model Users Guide, Version 1.0. GFDL Ocean Group Tech. Rep., No. 2.

Peters, H., M. C. Gregg, and J. M. Toole, 1988: On the parameterization of equatorial turbulence. *J. Geophys. Res.*, **93,** 1199–1218.

Philander, S. G. H., and R. C. Pacanowski, 1980: The generation of equatorial currents. *J. Geophys. Res.*, **85,** 1123–1136.

——, and A. D. Seigel, 1985: Simulation of the El Niño of 1982–83. *Coupled Ocean–Atmosphere Models, Elsevier Oceanogr. Ser.*, Vol. 40, J. C. J. Nihoul, Ed., Elsevier, 517–542.

Rosati, A., and K. Miyakoda, 1988: A general circulation model for upper ocean simulation. *J. Phys. Oceanogr.*, **18,** 1602–1626.

Sykes, R. I., W. S. Lewellen, and D. S. Henn, 1988: A numerical study of the development of cloud-street coupling. *J. Atmos. Sci.*, **45,** 556–569.